Am J Physiol Cell Physiol 318: C476–C485, 2020.
First published December 25, 2019; doi:10.1152/ajpcell.00221.2019.

RESEARCH ARTICLE | *Making Cell Culture More Physiological*

Bioenergetics underlying single-cell migration on aligned nanofiber scaffolds

Abinash Padhi,[1] Alexander H. Thomson,[2] Justin B. Perry,[2] Grace N. Davis,[2] Ryan P. McMillan,[2,6] Sandra Loesgen,[3] Elizabeth N. Kaweesa,[3] Rakesh Kapania,[4] Amrinder S. Nain,[1]* and David A. Brown[2,5,6]*

[1]*Department of Mechanical Engineering, Virginia Tech, Blacksburg, Virginia;* [2]*Department of Human Nutrition, Foods, and Exercise, Virginia Tech, Blacksburg, Virginia;* [3]*Department of Chemistry, Oregon State University, Corvallis, Oregon;* [4]*Department of Aerospace and Ocean Engineering, Virginia Tech, Blacksburg, Virginia;* [5]*Virginia Tech Center for Drug Discovery, Blacksburg, Virginia; and* [6]*Virginia Tech Metabolism Core, Blacksburg, Virginia*

Submitted 11 June 2019; accepted in final form 17 December 2019

Padhi A, Thomson AH, Perry JB, Davis GN, McMillan RP, Loesgen S, Kaweesa EN, Kapania R, Nain AS, Brown DA. Bioenergetics underlying single-cell migration on aligned nanofiber scaffolds. *Am J Physiol Cell Physiol* 318: C476–C485, 2020. First published December 25, 2019; doi:10.1152/ajpcell.00221.2019.— Cell migration is centrally involved in a myriad of physiological processes, including morphogenesis, wound healing, tissue repair, and metastatic growth. The bioenergetics that underlie migratory behavior are not fully understood, in part because of variations in cell culture media and utilization of experimental cell culture systems that do not model physiological connective extracellular fibrous networks. In this study, we evaluated the bioenergetics of C2C12 myoblast migration and force production on fibronectin-coated nanofiber scaffolds of controlled diameter and alignment, fabricated using a nonelectrospinning spinneret-based tunable engineered parameters (STEP) platform. The contribution of various metabolic pathways to cellular migration was determined using inhibitors of cellular respiration, ATP synthesis, glycolysis, or glucose uptake. Despite immediate effects on oxygen consumption, mitochondrial inhibition only modestly reduced cell migration velocity, whereas inhibitors of glycolysis and cellular glucose uptake led to striking decreases in migration. The migratory metabolic sensitivity was modifiable based on the substrates present in cell culture media. Cells cultured in galactose (instead of glucose) showed substantial migratory sensitivity to mitochondrial inhibition. We used nanonet force microscopy to determine the bioenergetic factors responsible for single-cell force production and observed that neither mitochondrial nor glycolytic inhibition altered single-cell force production. These data suggest that myoblast migration is heavily reliant on glycolysis in cells grown in conventional media. These studies have wide-ranging implications for the causes, consequences, and putative therapeutic treatments aimed at cellular migration.

bioenergetics; glycolysis; migration; mitochondria; single cell

INTRODUCTION

Cell migration is involved in a vast array of pathological and physiological processes, including cancer metastases (26), inflammation (7), tissue repair (22), and development (29). In muscle tissues, myoblast migration is associated with tissue growth and repair, with altered migratory behavior noted in diseases such as muscular dystrophy (32, 51). Migratory cells in vivo interact with the extracellular matrix (ECM), and little is known on the role of mitochondrial and glycolytic pathways affecting migration. This is in part the result of the complex cellular environment and the challenges in recapitulating the three-dimensional fibrous structures in laboratory settings in a controlled and repeatable fashion (9, 24). ECM structure influences cell geometry and is involved in transmission of both mechanical and biophysical cues to the cell (16). Cell migration has been traditionally studied using two-dimensional substrates, such as flat glass cover slips, which have yielded significant insights. Recently, three-dimensional ECM model systems [gels (14), cell-derived matrixes (12), and microgrooves (20)] provide a more integrative and physiological environment to study cellular behavior. In this study, we used the nonelectrospinning spinneret-based tunable engineered parameters (STEP) fiber manufacturing platform (23, 43, 45) to determine how bioenergetics in cell-three-dimensional fiber interactions influence cell migration and cell force production.

Glycolysis and mitochondrial oxidative phosphorylation are two major cellular metabolic processes that oxidize carbon sources from carbohydrates, proteins, and fatty acids into ATP. Glycolysis is a rapid yet low-yield pathway to generate ATP, whereas mitochondrial oxidative phosphorylation generates a substantially higher amount of ATP per mole of glucose, albeit at a slower rate. Previous studies have examined the energetics of cell migration and have shown that cell migration is predominantly glycolytic (4, 34). Although promising, most studies use glucose as the primary carbon source in the media, and many migration studies are conducted in cancer cell lines that exhibit their own unique metabolic characteristics, including the Warburg effect (39, 51).

In this study, we set out to determine the underlying bioenergetic contributors to cellular migration and force production in myoblast muscle cells cultured on suspended and aligned fibers. With this goal in mind, we altered carbon sources in the culture media and used a variety of pharmacological inhibitors to quantify the effects of various metabolic pathways on single-cell behavior.

METHODS

Cell lines and culture. C2C12 myoblasts (ATCC) were cultured and maintained in Dulbecco's modified Eagle's medium (DMEM; Fischer Scientific, Hampton, NH) using previously described protocols (5). Cells were cultured to 70–80% confluency before running experiments and were not used after passage 25. In glucose-enriched

* A. S. Nain and D. A. Brown contributed equally as co-senior authors on this work.

Address for reprint requests and other correspondence: D. A. Brown, Dept. of HNFE, Virginia Tech Metabolism Core, 1981 Kraft Dr., 1035 ILSB, Virginia Tech, Blacksburg, VA 24060 (e-mail: brownda@vt.edu).

conditions, the media contained 4 mM glucose and 1 mM sodium pyruvate. A separate subset of experiments was conducted with 10 mM galactose in the DMEM (0 mM glucose, 0 mM pyruvate, and 0 mM HEPES), supplemented with 15% FBS and 1% Penn-Strep (Fischer Scientific) for 14 days (3–4 passages). Migration and single-cell force production studies were performed in the same media in which cells were cultured, with inhibitors added at specific timepoints, as indicated below in *Microscopy for migration/force analysis* section. Pyruvate was excluded from the galactose-containing media using the rationale that this would force cells to rely on galactose catabolism, an approach with some limitations (see discussion below in *Study limitations* section). The osmolarity of the glucose- and galactose-enriched media was calculated to be around 330–335 mOsm/L. We cannot rule out that slight differences in our media osmolarity may have influenced the cellular growth conditions in glucose- versus galactose-grown cells.

Mitochondrial oxygen consumption rate and extracellular acidification rate. An Agilent Seahorse XF96 Extracellular Flux Analyzer (Agilent Technologies, Santa Clara, CA) was used to measure oxygen consumption rate (OCR) and extracellular acidification rate (ECAR) per our established techniques (5). C2C12 cells were seeded into the XF96 plate at a density of 15,000/well and incubated at 37°C (5% CO_2) for 24 h. Before the assay was run, cells were placed in Seahorse Base Media (pH 7.4). For OCR, a baseline respiration rate was measured, and antimycin-A (AMA: 2 μM) was added to determine the optimal concentration of mitochondrial respiratory (complex III) inhibition. ECAR was determined by monitoring the changes in pH after the sequential addition of glucose, oligomycin, and 2-deoxy-D-glucose (2DG, injections spaced 30 min apart). Cells were allowed to equilibrate in the SeaHorse chamber for 30 min, followed by injections of glucose (10 mM), the ATP synthase inhibitor oligomycin (2.5 μM; Millipore Sigma, Burlington, MA), and the glycolysis inhibitor 2DG (ranging from 0 to 75 mM). Glutamine (2 mM) was added to the XF Base Media before cell seeding. Cells were seeded at the same density as the OCR assay.

STEP fibrous substrate. We engineered a suspended network of polystyrene nanofibers using our established nonelectrospinning STEP technique (25, 50). Briefly, the migration scaffolds were made of parallel fibers of ~800 nm diameter deposited ~15 μm apart, with regions of orthogonally deposited fibers at the end. The orthogonal regions were fused at the interjections. The force nanonets were manufactured by depositing a layer of large-diameter fibers (~2 μm) deposited at a spacing of ~350 μm, and, orthogonal to it, smaller-diameter fibers (~250 nm) were deposited 10–12 μm apart.

Preparation of scaffolds. For both the migration and force studies, scaffolds were mounted on a six-well plate (MatTek, Ashland, MA) followed by sterilization using 3 mL of 70% ethanol for 10 min. After ethanol was aspirated, each well was washed two times with 3 mL of PBS. One hundred microliters of fibronectin (4 μg/mL) were then added, and scaffolds were incubated for 1 h in a 37°C CO_2 incubator before cell seeding at a density of 100,000/mL. After the addition of cells, scaffolds were placed in the incubator for 2 h to ensure cell adherence to the fibrous substrate followed by addition of 3 mL of media.

Microscopy for migration/force analysis. For migration and force studies, time-lapse videos of cells attached to STEP nanonets were generated using a ×20 (NA = 0.8) magnification objective on a Zeiss AxioObserver Z1 equipped with an incubation chamber. A preinhibition (control) measurement was taken, and cells were imaged every 4 min for 1 h. Next, cells were incubated with two different concentrations of a potent glycolytic inhibitor (2DG), glycolytic flux inhibitor [3-bromo pyruvic acid (3-BP); Millipore Sigma, Burlington, MA], a mitochondrial complex III inhibitor (AMA), and complex V inhibitor (oligomycin) for 1 h and subsequently imaged every 4 min for 6 h. Upon completion of the experiment, files were exported into Image J (version 1.8.0_66). For migration analysis, the displacement of the nucleus was tracked by selecting a single central point within the cell nucleus every 12 min. Cells that reversed direction were excluded from analysis. Cell migration velocities were then averaged every hour. For the force studies, fiber deflection was tracked every hour and then further analyzed using MATLAB (2017a) per our established methods (44, 49). Briefly, the small-diameter fibers (~250 nm) were modeled as beams with fixed-fixed boundary conditions. The error between deflection profiles predicted from finite element model and those obtained experimentally was minimized using an optimization framework while iteratively updating the force values. In our model, the force vectors originate at the paxillin focal adhesion sites and are directed along the F-actin stress fibers. The angles made by dominant stress fibers were determined using fixed stained fluorescent images of F-actin.

Glucose uptake analysis. Cellular glucose uptake was performed using our established protocols (3). C2C12 cells were plated at a confluency of 30–40% in a MatTek six-well plate. The cells were incubated with 1 μM mensacarcin, a compound known to influence mitochondrial function (28, 35), for 30 min in Krebs-Henseleit buffer containing (in mM) 118 NaCl, 24 $NaHCO_3$, 4.8 KCl, 2 $CaCl_2$, 1.2 $MgSO_4$, 1.2 KH_2PO_4, and 10 glucose. Radioactive 2DG (1.5 Ci/mL) and 2DG (10 μM) were placed in the media for an additional 30 min. Glucose uptake was quantified using a scintillation counter. In these studies, we validated that mensacarcin inhibited cellular glucose uptake, and, accordingly, this concentration (1 μM) was used in subsequent migration studies. Acute (within 6 h) mensacarcin treatment was not associated with any observable cellular death/toxicity. Longer-duration studies were conducted to determine any dose-dependent toxicity of mensacarcin by incubating the cells as described above for 24 h in mensacarcin doses ranging from 0.01 to 100 μM.

Lactate secretion assay. C2C12 cells assayed for lactate secretion were grown and plated in the same manner as the glucose uptake assays. On the day of the experiment, cells were incubated for 1 h in Krebs-Henseleit buffer containing (in mM) 118 NaCl, 24 $NaHCO_3$, 4.8 KCl, 2 $CaCl_2$, 1.2 $MgSO_4$, and 1.2 KH_2PO_4 and subsequently treated with 4.5 g/L glucose with either 0, 12 mM, or 50 mM 2-deoxyglucose for 1 h. Cell culture medium was then collected and lactate concentration was assessed via a commercially available kit (cat. no. A-108; Biomedical Research Service Center, University of Buffalo, State University of New York). Protein content per well was assessed via a bicinchoninic acid assay (Thermo Fisher, Waltham, MA) and lactate secretion was normalized to protein content.

High-resolution mitochondrial respiration. OCRs were determined using our previously established methods (2). Mitochondria were isolated from rat heart ventricle per our previously published protocols (47). The following substrates were added in succession after OCRs stabilized: glutamate (10 mM), malate (2 mM), rotenone (0.5 μM), succinate (10 mM), ADP (5 mM; Millipore Sigma, Burlington, MA), and rates of respiration were normalized to milligram of mitochondrial protein.

Statistical analysis. All data were analyzed and graphed using GraphPad Prism (V8) software. Data are presented as means ± SE, with dot plots representing individual data points to show raw data points, consistent with publication policies of the American Physiological Society. Migration and force measurements were analyzed using an ANOVA, followed by Tukey's post hoc. *F* statics are reported in the legends of each figure and were calculated using Brown-Forsythe. Significance values were reported if $P \leq 0.05$.

RESULTS

Mitochondrial inhibition modestly affects cell migration. We quantified the influence of inhibiting mitochondrial energetics on cell migration. Despite a clear and immediate inhibition of mitochondrial function (Fig. 1, *A* and *B*), there was a delayed and modest effect of respiratory chain inhibition on cell migration along fiber scaffolds. Representative images at 1 h

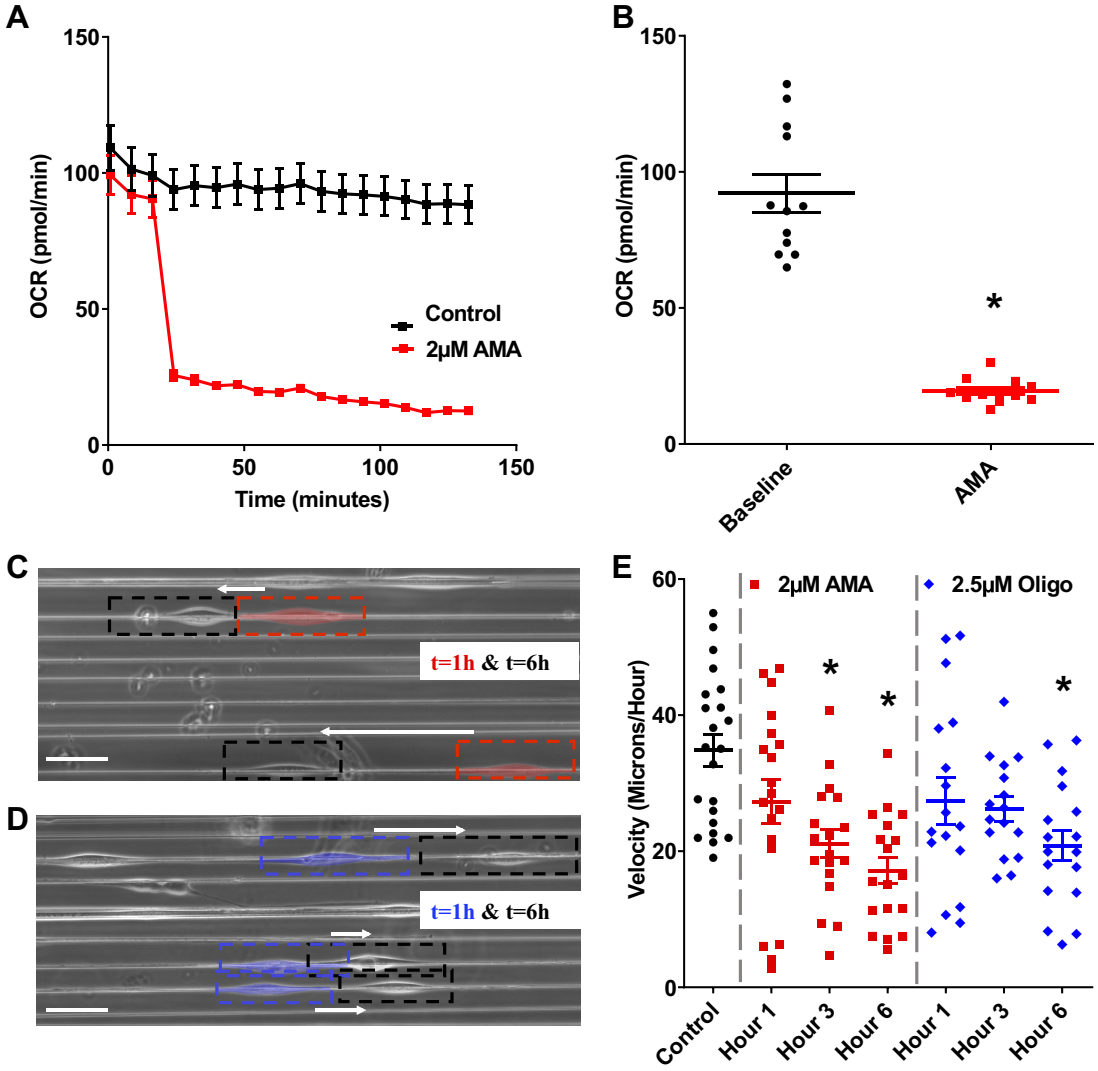

Fig. 1. Influence of inhibiting mitochondrial energetics on cell migration. *A*: oxygen consumption rate (OCR) in myoblasts displaying an immediate decrease in OCR after treatment with the complex III inhibitor antimycin-A (AMA; 2 μM). *B*: OCR data after 1 h of inhibition. *C*: representative time-lapse microscopy overlay images after the addition of 2 μM AMA. *D*: representative time-lapse microscopy overlay images after the addition of 2.5 μM oligomycin. Blue/red symbols indicates starting cell position (1 h), and black symbols indicates the same cell positioned after 6 h of treatment. Scale bar in *C* and *D*: 50 μm. *E*: quantification of change in migration velocity was overall modest and delayed following mitochondrial inhibition. ANOVA results: $F(6,120) = 2.129$, $P < 0.0001$. *$P < 0.05$ vs. control (n = 16–22 cells per group, n = 12–24 wells per group for Seahorse plate measurement) for individual group comparisons.

after inhibition (red cell, Fig. 1*C*) and at the end of 6 h postinhibition (black cell, Fig. 1*C*) indicate discernible cell movement despite clear inhibition of the respiratory chain with AMA. This can also be observed in Supplemental Video S1 (Supplemental Material is available at https://doi.org/10.6084/m9.figshare.8256641.v1).

We then inquired how inhibition of the ATP synthase (complex V) would alter cellular migration on our engineered scaffolds. Once again, there was only a modest effect of cells treated with oligomycin. Representative images at the onset of inhibition (blue cell, Fig. 1*D*) and at the end of 6 h (black cell, Fig. 1*D*) indicate cellular movement despite inhibiting mitochondrial ATP production. Quantified data in Fig. 1*E* indicate the modest and delayed effects of inhibiting mitochondrial bioenergetics on cellular migration along engineered nanofiber scaffolds.

Glycolysis inhibition significantly affects cell migration. Next, we determined the influence of aerobic glycolysis on cell migratory velocity. We first validated the dose-dependent efficacy of glycolytic inhibition (Fig. 2, *A* and *B*). The highest extent of glycolytic inhibition (reflected by a decline in ECAR after the 2DG injection) was observed at 2DG concentrations at or above 50 mM. Because tricarboxylic acid cycle-derived CO_2 has been shown to contribute to cellular acidification (31), lactate secretion data were also quantified as a direct measure of aerobic fermentation. Consistent with the ECAR data, lactate excretion was observed after treatment with 50 mM 2DG (Fig. 2*C*). Informed by these results, we determined the effects of moderate (12 mM 2DG) and higher (50 mM 2DG) glycolytic inhibition on cellular migration. Time-lapse images are presented in Fig. 2, *D–F*, as well as Supplemental Video S2. High doses of 2DG that substantially inhibited glycolysis essentially arrested cellular migration immediately, and this effect persisted for the duration of the 6-h procedure (Fig. 2, *D*, *E*, and *G*). Similar findings were observed with a different glycolytic inhibitor

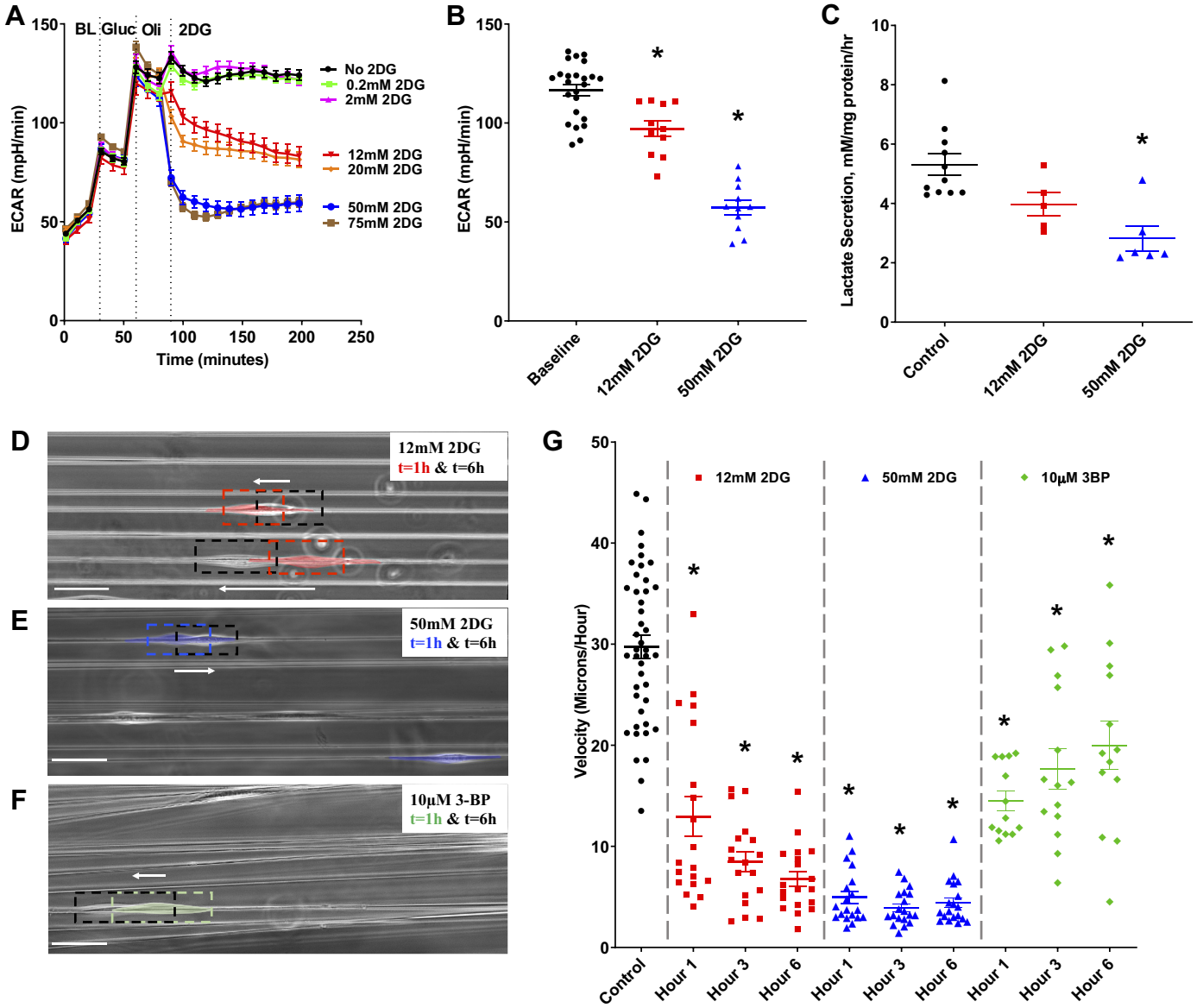

Fig. 2. Quantifying the role of glycolysis in cell migration. *A*: extracellular acidification rate (ECAR) showing a dose-dependent inhibition of glycolysis by 2-deoxyglucose (2DG). *B*: ECAR data after 1 h of inhibition. *C*: normalized lactate secretion decreased with increasing 2DG concentration. *D*: representative time-lapse microscopy overlay images after the addition of 12 mM 2DG. *E*: representative time-lapse microscopy overlay images after the addition of 50 mM 2DG. *F*: representative time-lapse microscopy overlay images after the addition of 10 μM 3-bromopyruvic acid (3-BP). Red/blue/green cell indicates the starting cell position (1 h), and black cell indicates the same cell positioned 6 h later. Scale bar in *D*–*F*: 50 μm. *G*: quantification of the changes in cellular migratory velocity following moderate and severe inhibition of glycolysis with 2DG and 3-BP. BL, baseline; Gluc, glucose; Oli, oligomycin (a complex V inhibitor). ANOVA results: $F(2,43) = 72.58$, $P < 0.00010$ (*B*); $F(2,19) = 10.20$, $P = 0.0010$ (*C*); and $F(9,186) = 59.03$, $P < 0.0001$ (*E*). *$P < 0.05$ vs. control (n = 13–43 cells per group, n = 9–22 wells per group for SeaHorse plate measurement).

(3-BP), which also led to a statistically significant inhibition of migration (Fig. 2, *F* and *G*).

Increasing cell reliance on mitochondrial respiration with galactose. Given that most cells grown in glucose-enriched culture media predominantly rely on aerobic glycolysis for energetic needs (10), we derived a series of studies where we removed glucose and sodium pyruvate from the cell culture media and supplemented with 10 mM galactose. This paradigm is postulated to force cellular utilization of mitochondria for energy generation (1, 30, 38), although this assumption has limitations (see *Study limitations*).

Migratory data from galactose-grown cells are presented in Fig. 3. Interestingly, unlike cells grown in conventional media, cellular migratory behavior in galactose-grown cells was quickly and substantially halted with mitochondrial inhibition.

Influence of glucose availability on cell migration. Next, we examined the effects of glucose availability on migration velocity. We used two parallel approaches to determine the effects of cellular glucose catabolism on migratory velocity (Fig. 4). The first approach used a novel compound, mensacarcin, a highly oxygenated polyketide isolated from *Streptomyces* bacteria (35). This compound has previously been shown to influence mitochondrial function, although it was not clear if this was a direct or indirect effect of the compound on cellular metabolism. In the second approach we omitted glucose from the media during the experiments.

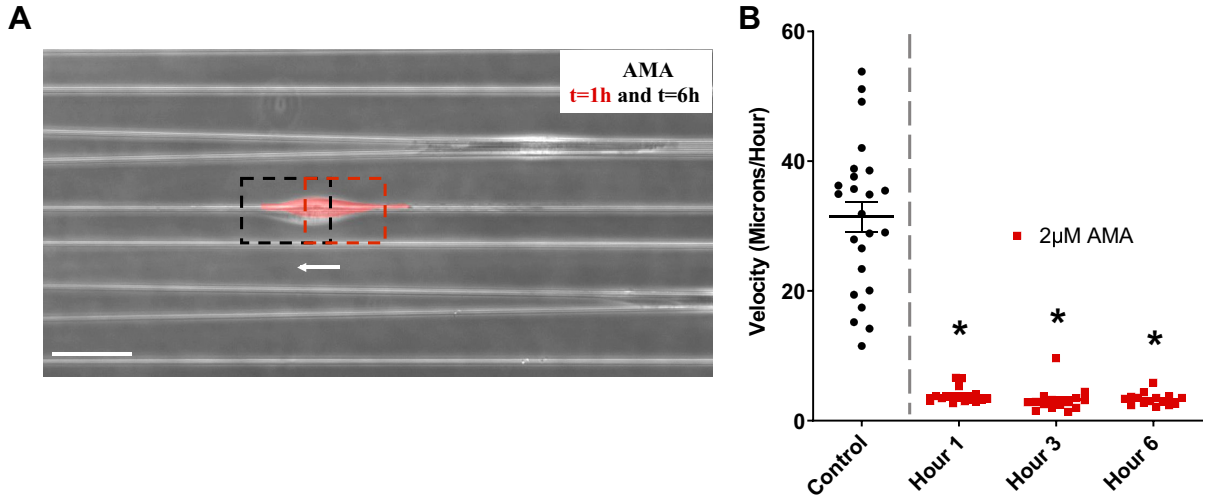

Fig. 3. Influence of cell culture media substrates on bioenergetic migratory sensitivity. *A*: representative time-lapse microscopy overlay images of galactose-grown cells treated with the mitochondrial complex III inhibitor antimycin-A (AMA; 2 μM). Scale bar: 50 μm. *B*: quantification of cellular migration velocity after treatment. Unlike cells grown in conventional (glucose-enriched) media, mitochondrial inhibition substantially blunted cellular migratory behavior in galactose-grown cells. *$P < 0.05$ vs. control ($n = 15$–24 cells per group). ANOVA results: $F(3,65) = 83.52$, $P < 0.0001$.

Migration velocity in cells treated with mensacarcin (Fig. 4, *A* and *B*) or in the absence of glucose (Fig. 4, *A* and *C*) was significantly slowed. Using radiolabeled substrate assays, we found that mensacarcin substantially blunted cellular glucose uptake (Fig. 4*D*). Interestingly, there were no observable effects of mensacarcin on mitochondrial function regardless of the substrates present in isolated mitochondria (Fig. 4*E*), confirming that the immediate actions of this compound on migratory velocity appear to be "upstream" of mitochondrial metabolism. We did not observe any discernable toxicity effects of mensacarcin during the first 6-h window. However, prolonged (24-h) mensacarcin exposure led to a dose-dependent decrease in cell viability (Fig. 4*F*).

Bioenergetic contribution to single-cell force production. We also determined the energetics of C2C12 single-cell force production. We used fused-fiber nanonet-based nanonet force microscopy (NFM) to measure single-cell forces (Fig. 5*A*). NFM uses force vectors that originate from focal adhesion cluster sites and are directed along tension-bearing F-actin stress fibers (Fig. 5*A*; see Refs. 44 and 49). Representative cells on nanonet force sensors in the presence of AMA and 2DG ae shown in Fig. 5, *B* and *C*. F-actin stress fiber angle measurements from fixed immunofluorescence staining showed slightly higher angles for cells treated with 2DG, but the forces for both drug conditions of mitochondrial (2 μM AMA) and glycolytic (50 mM 2DG) inhibition had an indiscernible effect on C2C12 force production for the 6 h following treatment (Fig. 5, *D* and *E*). C2C12 cells grown in galactose had similar preinhibition force measurements (94 nN; $n = 11$ cells) compared with conventionally grown C2C12 cells (107 nN; $n = 20$ cells). Cells grown in galactose detached from one or both of the fibers after metabolic inhibition, thus preventing force calculations.

DISCUSSION

Overview. In this study, we determined the bioenergetic contributors to C2C12 cell migration and force production on ECM-mimicking fibers. To the best of our knowledge, there are several novel aspects to our study. First, we demonstrated that, despite having rapid profound inhibitory effects on mitochondria, chemical inhibitors of oxidative phosphorylation had a very modest effect on migration velocity in the time frame studied. Second, glucose uptake and utilization appear to be critical to support migratory behavior. Third, we found that the bioenergetic contributors to cell migration can be modulated, specifically by incubating cells in galactose, which sensitized cells to mitochondrial inhibitors. Finally, we provide novel insight into single-cell force production in our models, where neither mitochondrial nor glycolytic inhibition altered cellular force production during the time course examined.

Reliance on aerobic glycolysis for cellular migration in C2C12 cells. Our observation that glucose uptake and aerobic glycolysis were major contributors to cell migration complements recent studies across experimental models. Inhibition of glycolysis has been shown to reduce migratory behavior in breast cancer cells (13), endothelial cells (and subsequently angiogenesis; see Ref. 39), and glioblastoma cells (17, 40).

Inhibition of mitochondrial bioenergetics had a modest, and much more delayed, effect on C2C12 migration. These data are generally consistent with other studies, indicating that, across models, glycolytically derived ATP ostensibly generated in close proximity to active cytoskeletal proteins is overwhelmingly responsible for cellular motility (46). Interestingly, across these studies, the metabolic substrate for cells is primarily glucose. We next determined how carbon sources within cell culture media influenced the susceptibility of migratory behavior to bioenergetic inhibitors.

Inhibiting cellular migration by limiting glucose availability. As it became increasingly clear that glucose-grown cells rely heavily on glucose catabolism for migration, we tested the direct effects of removing glucose availability on C2C12 migration. Omission of glucose had rapid and significant effects on cellular migration, indicating that intracellular glycogen stores are very limited, essentially exhausted within an hour as migration was substantially blunted. We also used a new approach to limit cellular glucose uptake with the novel com-

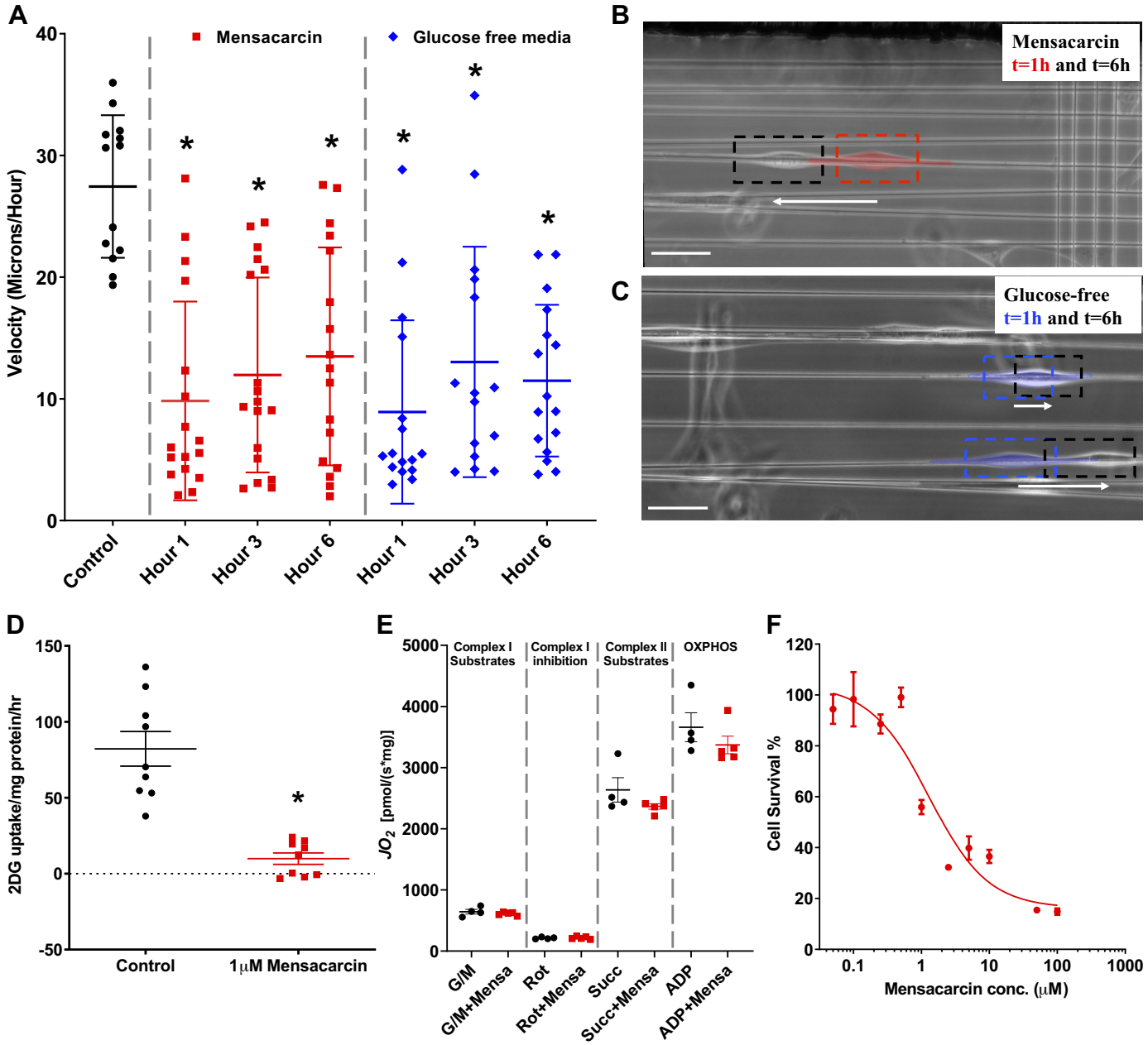

Fig. 4. Glucose dependency of cellular migration. *A*: mitigated migration velocities observed in the presence of the novel compound mensacarcin or in media devoid of glucose. *B*: time-lapse microscopy overlay images of cellular migration before (red) and after (black) treatment with mensacarcin, an inhibitor of glucose uptake, which significantly blunted migratory velocities . *C*: time-lapse microscopy overlay images of cellular migration before (blue) and after (black) treatment in media devoid of glucose, which significantly blunted migratory velocities. Scale bar in *B* and *C*: 50 μm. *D*: inhibition of C2C12 cellular glucose uptake with mensacarcin. *E*: no discernible effect of mensacarcin on isolated mitochondria, regardless of the substrate conditions, was observed after confirming that mensacarcin appeared to be influencing cellular glucose uptake and not mitochondrial respiration. *F*: dose-dependent effects of mensacarcin on cell viability over 24 h. G/M, glutamate/malate; Rot, rotenone; Succ, succinate. ANOVA results: $F(6,10) = 8.56$, $P < 0.0001$ (*A*). *$P < 0.05$ vs. control (n = 13–18 per group).

pound mensacarcin. Mensacarcin is a recently described highly oxygenated polyketide recently isolated from *Streptomyces* bacteria (35) that is currently being tested in melanoma cell models. In this study we demonstrated that mensacarcin rapidly reduces cellular glucose uptake without being acutely cytotoxic, which resulted in substantial blunting of migratory velocity. Our results suggest that glycolysis is necessary for migration and that the carbon sources (glucose) must be constantly replenished for cells to continue moving. Mensacarcin adds to the small group of complex natural products that influence cellular uptake (27). Its inhibitory activity in cellular migration in these studies further supports investigation in cancer cell lines.

Bioenergetics underlying migration in galactose-grown cells. Cells grown in culture often have minimal energy demands, mostly needing ATP for proliferation, protein turnover, and maintenance of membrane gradients. It seems intuitive that cultured cells rely primarily on the rapid but quantitatively

small ATP content generated by aerobic glycolysis. Cells/tissues in vivo (notably striated muscle) have exponentially higher energy demands, and, accordingly, the reliance on mitochondrial energy generation is postulated to be much greater than quiescent cultured cells. We next determined the bioenergetic contributors to migratory behavior in cells forced to rely on mitochondrial oxidative phosphorylation. We cultured cells in glucose/pyruvate-free media that was supple-

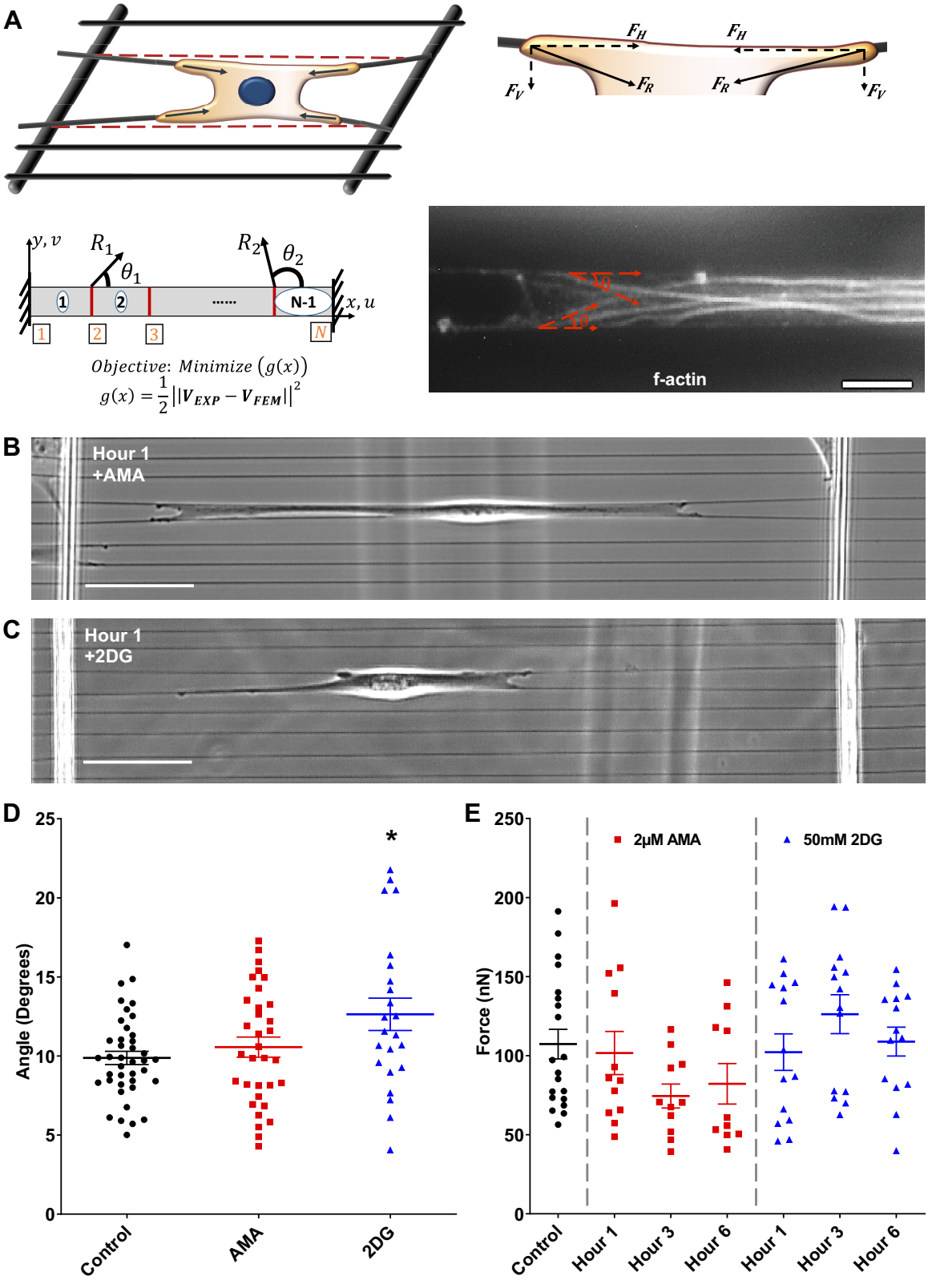

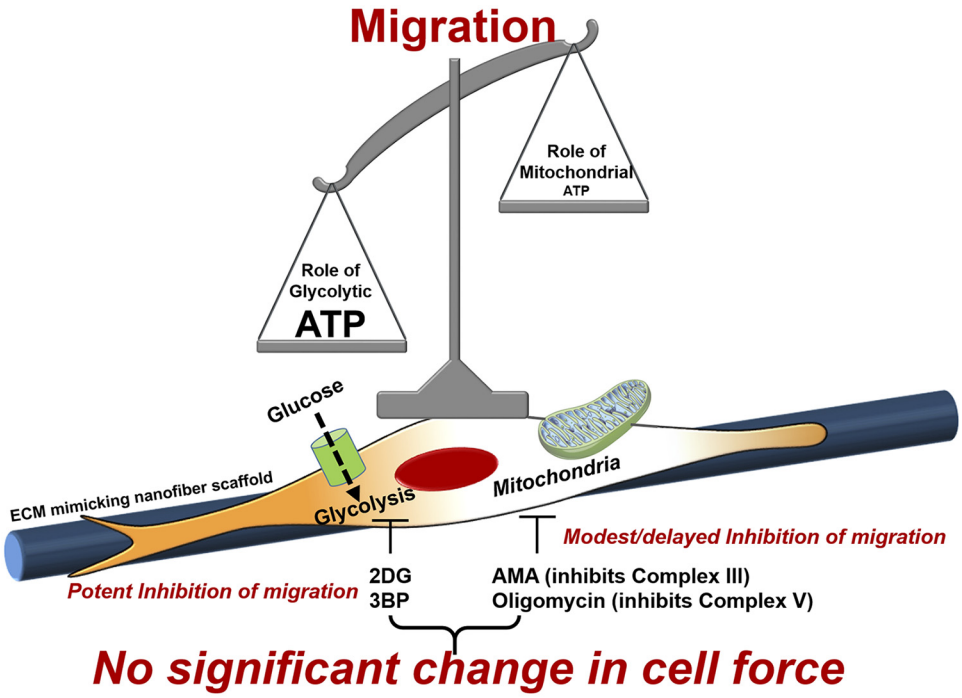

Fig. 6. Summary overview of bioenergetic pathways studied in migration studies depicting the dominant contribution of glycolytic energy production in driving cell migration. No significant alterations in single-cell force production were observed by inhibiting glycolysis or oxidative phosphorylation in the time frame studied. 2DG, 2-deoxyglucose; 3-BP, 3-bromopyruvic acid; AMA, antimycin-A; ECM, extracellular matrix.

mented with galactose. Galactose supplementation has previously been shown to result in cellular upregulation of mitochondrial proteins, heightened sensitivity to mitochondrial toxicants, and an increased reliance on oxidative phosphorylation (11, 30, 38).

Our novel findings that galactose-supplemented cells showed augmented migratory inhibition to mitochondrial inhibitors has a number of implications, notably that physiological movement of cells in vivo (versus grown in vitro) may be augmented (or arrested) by treatments aimed at mitochondria. These data indicate that the paradigms employed herein (physiologically relevant ECM scaffolds coupled with substrates that require mitochondrial oxidative phosphorylation) reflect a platform with higher likelihood to discover mitochondria-directed therapies targeting cellular migration in vivo than conventional approaches. While promising, there are also clear limitations with the use of galactose in vitro, which is expanded upon below in the *Study limitations* section.

Bioenergetics underlying single-cell force production. We coupled our studies on cellular migration with experiments aimed to advance our understanding at how single cells are able to generate forces. Cells generate force (inside out) and also respond to forces that originate outside the extracellular matrix (ECM) (outside in). Cells pull directionally, and these forces are then transmitted back to the substrate by focal adhesions (41). Because cells are able to sense and respond to changes in fiber curvature and structural stiffness (45), deflection of these fibers can be converted to a force measurement (18, 42, 44, 49). Our results showed that, even in the presence of energetic inhibition, the cells were able to sustain a similar amount of force, suggesting that tonic C2C12 force production is a low-energy turnover process, perhaps analogous to the "latch state" observed in other muscle types. Studies conducted in muscle have shown that force is maintained with minimal energy (ATP) consumption (48). We caution that our in vitro fibrous assay attempts to recapitulate the complex native environment in which few cell attachment points (large pore size) force cells to make contact with only a few fibers (12, 15, 19). Further improvements in density, organization, and size of fibers will provide a comprehensive understanding in energetic pathways used by cells exhibiting diverse modes of cell migration in varying shapes (23) and invasion modes (single versus collective) (43).

Study limitations. The use of both galactose and 2DG provides insight into cellular metabolic pathways, although there are clear limitations with the use of these compounds. Galactose treatment has been shown to mediate cellular glutamine catabolism instead of galactose catabolism (36), so our studies using galactose as a carbon substrate must be interpreted with caution, especially since the media contained no glucose to

Fig. 5. Bioenergetic contribution to single-cell force production. *A*: graphical depiction of the spinneret-based tunable engineered parameters (STEP) platform and the variables used to calculate single-cell force production based on fiber deflection. Fiber is modeled as a beam with fixed ends and discretized into N-1 elements with *N* nodes. Displacement in the *y*-direction is *v* and in the *x*-direction is *u*. Resultant force vectors $\mathbf{R}_1$ and $\mathbf{R}_2$ act at angles θ_1 and θ_2, respectively. $\mathbf{F}_H$ and $\mathbf{F}_V$ are the horizontal and vertical components of forces, respectively., and $\mathbf{F}_R$ is the resultant force vector. $\mathbf{V}_{EXP}$ is the vector of vertical displacements (v_i) generated after interpolating the experimental vertical displacements, and $\mathbf{V}_{FEM}$ is the vector of computational vertical displacements obtained from the finite element model. *B*: representative image of cells treated with the complex III inhibitor antimycin-A (AMA). *C*: representative image of cells in 2-deoxyglucose (2DG). *D*: the F-actin stress fiber angle data were quantified (*$P < 0.05$; $n = 23$–40 stress fibers per group). *E*: time-dependent force calculations (in nN) are presented based on fiber deflections. There were no significant effects of either mitochondrial or glycolytic inhibition on single-cell force production ($n = 10$–20 cells per group). Scale bar: 50 μm. ANOVA results: $F(2,93) = 4.28$, $P = 0.0167$.

support a UDP-glucose pool (Leloir pathway). We also did not determine if galactose-grown cells had higher maximal glycolytic flux in our studies. Furthermore, 2DG has been shown to impair respiration and likely influences cellular metabolism via multiple pathways (6, 21), again requiring thoughtful interpretation of the data.

Summary and future directions. Our studies highlight the importance of cellular substrates and the physical environment as critical determinants to cellular migration. The combination of physiologically relevant scaffolds with substrate conditions that may better reflect energy demands in vivo have provided new insight into the bioenergetics that underlie cellular migration. Conventionally grown cells rely largely on aerobic glycolysis coupled with *trans*-cellular glucose replenishment for migration, whereas cells cultured in galactose become more reliant on oxidative phosphorylation for migration. Maintenance of cell force does not appear to require the similar degree of energy turnover as migration (Fig. 6). Future studies determining cellular energy requirements for specific phases of the cell migration cycle, determining how glycolytic proteins may comigrate with cellular protrusions (8, 25, 33, 37), and determining the changes in bioenergetics when cells are adhered to fibers of varying sizes and geometries will advance our understanding of this exciting field.

ACKNOWLEDGMENTS

We are grateful to Dr. Axel Zeeck and Hans-Peter Kroll (Bioviotica) for providing mensacarcin.

Correspondence may also be addressed to A. S. Nain (e-mail: nain@vt.edu).

Present address of S. Loesgen and E. N. Kaweesa: Whitney Laboratory for Marine Bioscience and Department of Chemistry, University of Florida, St. Augustine, Florida.

GRANTS

This work was supported by NIH National Heart, Lung, and Blood Institute Grant HL-123647 (to D. A. Brown), U.S. Department of Agriculture National Institute of Food and Agriculture Hatch Project Grant 1017927 (to D. A. Brown), and National Science Foundation Grants 1437101 and 1762634 (to A. S. Nain).

DISCLOSURES

No conflicts of interest, financial or otherwise, are declared by the authors.

AUTHOR CONTRIBUTIONS

A.P., A.H.T., J.B.P., G.N.D., R.P.M., S.L., E.N.K., A.S.N., and D.A.B. conceived and designed research; A.P., A.H.T., J.B.P., G.N.D., R.P.M., S.L., E.N.K., R.K., A.S.N., and D.A.B. performed experiments; A.P., A.H.T., J.B.P., G.N.D., R.P.M., S.L., E.N.K., R.K., A.S.N., and D.A.B. analyzed data; A.P., A.H.T., J.B.P., G.N.D., R.P.M., S.L., E.N.K., R.K., A.S.N., and D.A.B. interpreted results of experiments; A.P., A.H.T., J.B.P., G.N.D., R.P.M., S.L., E.N.K., R.K., A.S.N., and D.A.B. prepared figures; A.P., A.H.T., R.P.M., S.L., A.S.N., and D.A.B. drafted manuscript; A.P., A.H.T., R.P.M., S.L., E.N.K., R.K., A.S.N., and D.A.B. edited and revised manuscript; A.P., A.H.T., J.B.P., G.N.D., R.P.M., S.L., E.N.K., R.K., A.S.N., and D.A.B. approved final version of manuscript.

REFERENCES

1. **Aguer C, Gambarotta D, Mailloux RJ, Moffat C, Dent R, McPherson R, Harper ME.** Galactose enhances oxidative metabolism and reveals mitochondrial dysfunction in human primary muscle cells. *PLoS One* 6: e28536, 2011. doi:10.1371/journal.pone.0028536.
2. **Alleman RJ, Tsang AM, Ryan TE, Patteson DJ, McClung JM, Spangenburg EE, Shaikh SR, Neufer PD, Brown DA.** Exercise-induced protection against reperfusion arrhythmia involves stabilization of mitochondrial energetics. *Am J Physiol Heart Circ Physiol* 310: H1360–H1370, 2016. doi:10.1152/ajpheart.00858.2015.
3. **Anderson AS, Roberts PC, Frisard MI, McMillan RP, Brown TJ, Lawless MH, Hulver MW, Schmelz EM.** Metabolic changes during ovarian cancer progression as targets for sphingosine treatment. *Exp Cell Res* 319: 1431–1442, 2013. doi:10.1016/j.yexcr.2013.02.017.
4. **Arseneault R, Chien A, Newington JT, Rappon T, Harris R, Cumming RC.** Attenuation of LDHA expression in cancer cells leads to redox-dependent alterations in cytoskeletal structure and cell migration. *Cancer Lett* 338: 255–266, 2013. doi:10.1016/j.canlet.2013.03.034.
5. **Bitner BF, Ray JD, Kener KB, Herring JA, Tueller JA, Johnson DK, Tellez Freitas CM, Fausnacht DW, Allen ME, Thomson AH, Weber KS, McMillan RP, Hulver MW, Brown DA, Tessem JS, Neilson AP.** Common gut microbial metabolites of dietary flavonoids exert potent protective activities in β-cells and skeletal muscle cells. *J Nutr Biochem* 62: 95–107, 2018. doi:10.1016/j.jnutbio.2018.09.004.
6. **Brand MD, Nicholls DG.** Assessing mitochondrial dysfunction in cells. *Biochem J* 435: 297–312, 2011. doi:10.1042/BJ20110162.
7. **Burn T, Alvarez JI.** Reverse transendothelial cell migration in inflammation: to help or to hinder? *Cell Mol Life Sci* 74: 1871–1881, 2017. doi:10.1007/s00018-016-2444-2.
8. **Carey SP, Goldblatt ZE, Martin KE, Romero B, Williams RM, Reinhart-King CA.** Local extracellular matrix alignment directs cellular protrusion dynamics and migration through Rac1 and FAK. *Integr Biol* 8: 821–835, 2016. doi:10.1039/C6IB00030D.
9. **Charras G, Sahai E.** Physical influences of the extracellular environment on cell migration. *Nat Rev Mol Cell Biol* 15: 813–824, 2014. doi:10.1038/nrm3897.
10. **Diaz-Ruiz R, Rigoulet M, Devin A.** The Warburg and Crabtree effects: On the origin of cancer cell energy metabolism and of yeast glucose repression. *Biochim Biophys Acta* 1807: 568–576, 2011. doi:10.1016/j.bbabio.2010.08.010.
11. **Dott W, Mistry P, Wright J, Cain K, Herbert KE.** Modulation of mitochondrial bioenergetics in a skeletal muscle cell line model of mitochondrial toxicity. *Redox Biol* 2: 224–233, 2014. doi:10.1016/j.redox.2013.12.028.
12. **Doyle AD, Wang FW, Matsumoto K, Yamada KM.** One-dimensional topography underlies three-dimensional fibrillar cell migration. *J Cell Biol* 184: 481–490, 2009. doi:10.1083/jcb.200810041.
13. **Feng X, Wang P, Liu Q, Zhang T, Mai B, Wang X.** Glycolytic inhibitors 2-deoxyglucose and 3-bromopyruvate synergize with photodynamic therapy respectively to inhibit cell migration. *J Bioenerg Biomembr* 47: 189–197, 2015. doi:10.1007/s10863-015-9604-1.
14. **Fraley SI, Feng Y, Krishnamurthy R, Kim D-H, Celedon A, Longmore GD, Wirtz D.** A distinctive role for focal adhesion proteins in three-dimensional cell motility. *Nat Cell Biol* 12: 598–604, 2010. doi:10.1038/ncb2062.
15. **Friedl P, Wolf K.** Plasticity of cell migration: a multiscale tuning model. *J Cell Biol* 188: 11–19, 2010. doi:10.1083/jcb.200909003.
16. **Guilak F, Cohen DM, Estes BT, Gimble JM, Liedtke W, Chen CS.** Control of stem cell fate by physical interactions with the extracellular matrix. *Cell Stem Cell* 5: 17–26, 2009. doi:10.1016/j.stem.2009.06.016.
17. **Gupta P, Jagavelu K, Mishra DP.** Inhibition of NADPH oxidase-4 potentiates 2-deoxy-D-glucose-induced suppression of glycolysis, migration, and invasion in glioblastoma cells: role of the Akt/HIF1α/HK-2 signaling axis. *Antioxid Redox Signal* 23: 665–681, 2015. doi:10.1089/ars.2014.5973.
18. **Hall A, Chan P, Sheets K, Apperson M, Delaughter C, Gleason TG, Phillippi JA, Nain A.** Nanonet force microscopy for measuring forces in single smooth muscle cells of the human aorta. *Mol Biol Cell* 28: 1894–1900, 2017. doi:10.1091/mbc.e17-01-0053.
19. **Harley BAC, Kim H-D, Zaman MH, Yannas IV, Lauffenburger DA, Gibson LJ.** Microarchitecture of three-dimensional scaffolds influences cell migration behavior via junction interactions. *Biophys J* 95: 4013–4024, 2008. doi:10.1529/biophysj.107.122598.
20. **Hung W-C, Chen S-H, Paul CD, Stroka KM, Lo Y-C, Yang JT, Konstantopoulos K.** Distinct signaling mechanisms regulate migration in unconfined versus confined spaces. *J Cell Biol* 202: 807–824, 2013. doi:10.1083/jcb.201302132.
21. **Ibsen KH, Coe EL, McKEE RW.** A comparison of the respiratory inhibitions induced by D-glucose and 2-deoxy-D-glucose in Ehrlich ascites carcinoma cells. *Cancer Res* 22: 182–186, 1962.
22. **Ilina O, Friedl P.** Mechanisms of collective cell migration at a glance. *J Cell Sci* 122: 3203–3208, 2009. doi:10.1242/jcs.036525.
23. **Jana A, Nookaew I, Singh J, Behkam B, Franco AT, Nain AS.** Crosshatch nanofiber networks of tunable interfiber spacing induce plas-

ticity in cell migration and cytoskeletal response. *FASEB J* 33: 10618–10632, 2019. doi:10.1096/fj.201900131R.
24. **Keely P, Nain A.** Capturing relevant extracellular matrices for investigating cell migration. *F1000 Res* 4: 1408, 2015. doi:10.12688/f1000research.6623.1.
25. **Koons B, Sharma P, Ye Z, Mukherjee A, Lee MH, Wirtz D, Behkam B, Nain AS.** Cancer protrusions on a tightrope: nanofiber curvature contrast quantitates single protrusion dynamics. *ACS Nano* 11: 12037–12048, 2017. doi:10.1021/acsnano.7b04567.
26. **Kumar S, Weaver VM.** Mechanics, malignancy, and metastasis: the force journey of a tumor cell. *Cancer Metastasis Rev* 28: 113–127, 2009. doi:10.1007/s10555-008-9173-4.
27. **Kuo S-C, Lampen JO.** Action of cytochalasin A, a sulfhydryl-reactive agent, on sugar metabolism and membrane-bound adenosine triphosphatase of yeast. *Biochim Biophys Acta* 389: 145–153, 1975. doi:10.1016/0005-2736(75)90392-2.
28. **Maier S, Pflüger T, Loesgen S, Asmus K, Brötz E, Paululat T, Zeeck A, Andrade S, Bechthold A.** Insights into the bioactivity of mensacarcin and epoxide formation by MsnO8. *ChemBioChem* 15: 749–756, 2014. doi:10.1002/cbic.201300704.
29. **Mammoto T, Ingber DE.** Mechanical control of tissue and organ development. *Development* 137: 1407–1420, 2010. doi:10.1242/dev.024166.
30. **Marroquin LD, Hynes J, Dykens JA, Jamieson JD, Will Y.** Circumventing the Crabtree effect: replacing media glucose with galactose increases susceptibility of HepG2 cells to mitochondrial toxicants. *Toxicol Sci* 97: 539–547, 2007. doi:10.1093/toxsci/kfm052.
31. **Mookerjee SA, Goncalves RLS, Gerencser AA, Nicholls DG, Brand MD.** The contributions of respiration and glycolysis to extracellular acid production. *Biochim Biophys Acta* 1847: 171–181, 2015. doi:10.1016/j.bbabio.2014.10.005.
32. **Morgan J, Rouche A, Bausero P, Houssaïni A, Gross J, Fiszman MY, Alameddine HS.** MMP-9 overexpression improves myogenic cell migration and engraftment. *Muscle Nerve* 42: 584–595, 2010. doi:10.1002/mus.21737.
33. **Mukherjee A, Behkam B, Nain AS.** Cancer cells sense fibers by coiling on them in a curvature-dependent manner. *iScience* 19: 905–915, 2019. doi:10.1016/j.isci.2019.08.023.
34. **Mustafa EH, Mahmoud HT, Al-Hudhud MY, Abdalla MY, Ahmad IM, Yasin SR, Elkarmi AZ, Tahtamouni LH.** 2-deoxy-D-glucose synergizes with doxorubicin or L-buthionine sulfoximine to reduce adhesion and migration of breast cancer cells. *Asian Pac J Cancer Prev* 16: 3213–3222, 2015. doi:10.7314/APJCP.2015.16.8.3213.
35. **Plitzko B, Kaweesa EN, Loesgen S.** The natural product mensacarcin induces mitochondrial toxicity and apoptosis in melanoma cells. *J Biol Chem* 292: 21102–21116, 2017. doi:10.1074/jbc.M116.774836.
36. **Reitzer LJ, Wice BM, Kennell D.** Evidence that glutamine, not sugar, is the major energy source for cultured HeLa cells. *J Biol Chem* 254: 2669–2676, 1979.
37. **Riching KM, Cox BL, Salick MR, Pehlke C, Riching AS, Ponik SM, Bass BR, Crone WC, Jiang Y, Weaver AM, Eliceiri KW, Keely PJ.** 3D collagen alignment limits protrusions to enhance breast cancer cell persistence. *Biophys J* 107: 2546–2558, 2014. doi:10.1016/j.bpj.2014.10.035.
38. **Rossignol R, Gilkerson R, Aggeler R, Yamagata K, Remington SJ, Capaldi RA.** Energy substrate modulates mitochondrial structure and oxidative capacity in cancer cells. *Cancer Res* 64: 985–993, 2004. doi:10.1158/0008-5472.CAN-03-1101.
39. **San-Millán I, Brooks GA.** Reexamining cancer metabolism: lactate production for carcinogenesis could be the purpose and explanation of the Warburg Effect. *Carcinogenesis* 38: 119–133, 2017. doi:10.1093/carcin/bgw127.
40. **Schoors S, De Bock K, Cantelmo AR, Georgiadou M, Ghesquière B, Cauwenberghs S, Kuchnio A, Wong BW, Quaegebeur A, Goveia J, Bifari F, Wang X, Blanco R, Tembuyser B, Cornelissen I, Bouché A, Vinckier S, Diaz-Moralli S, Gerhardt H, Telang S, Cascante M, Chesney J, Dewerchin M, Carmeliet P.** Partial and transient reduction of glycolysis by PFKFB3 blockade reduces pathological angiogenesis. *Cell Metab* 19: 37–48, 2014. doi:10.1016/j.cmet.2013.11.008.
41. **Schwarz US, Safran SA.** Physics of adherent cells. *Rev Mod Phys* 85: 1327–1381, 2013. doi:10.1103/RevModPhys.85.1327.
42. **Sharma P, Kim A, Gill A, Wang J, Sheets K, Behkam B, Nain AS.** Aligned and suspended fiber force probes for drug testing at single cell resolution. *Biofabrication* 6: 045006, 2014. doi:10.1088/1758-5082/6/4/045006.
43. **Sharma P, Ng C, Jana A, Padhi A, Szymanski P, Lee JSH, Behkam B, Nain AS.** Aligned fibers direct collective cell migration to engineer closing and nonclosing wound gaps. *Mol Biol Cell* 28: 2579–2588, 2017. doi:10.1091/mbc.e17-05-0305.
44. **Sheets K, Wang J, Zhao W, Kapania R, Nain AS.** Nanonet force microscopy for measuring cell forces. *Biophys J* 111: 197–207, 2016. doi:10.1016/j.bpj.2016.05.031.
45. **Sheets K, Wunsch S, Ng C, Nain AS.** Shape-dependent cell migration and focal adhesion organization on suspended and aligned nanofiber scaffolds. *Acta Biomater* 9: 7169–7177, 2013. doi:10.1016/j.actbio.2013.03.042.
46. **Shiraishi T, Verdone JE, Huang J, Kahlert UD, Hernandez JR, Torga G, Zarif JC, Epstein T, Gatenby R, McCartney A, Elisseeff JH, Mooney SM, An SS, Pienta KJ.** Glycolysis is the primary bioenergetic pathway for cell motility and cytoskeletal remodeling in human prostate and breast cancer cells. *Oncotarget* 6: 130–143, 2015. doi:10.18632/oncotarget.2766.
47. **Sloan RC, Moukdar F, Frasier CR, Patel HD, Bostian PA, Lust RM, Brown DA.** Mitochondrial permeability transition in the diabetic heart: contributions of thiol redox state and mitochondrial calcium to augmented reperfusion injury. *J Mol Cell Cardiol* 52: 1009–1018, 2012. doi:10.1016/j.yjmcc.2012.02.009.
48. **Tanaka H, Homma K, White HD, Yanagida T, Ikebe M.** Smooth muscle myosin phosphorylated at single head shows sustained mechanical activity. *J Biol Chem* 283: 15611–15618, 2008. doi:10.1074/jbc.M710597200.
49. **Tu-Sekine B, Padhi A, Jin S, Kalyan S, Singh K, Apperson M, Kapania R, Hur SC, Nain A, Kim SF.** Inositol polyphosphate multikinase is a metformin target that regulates cell migration. *FASEB J* 33: 14137–14146, 2019. doi:10.1096/fj.201900717RR.
50. **Wang J, Nain AS.** Suspended micro/nanofiber hierarchical biological scaffolds fabricated using non-electrospinning STEP technique. *Langmuir* 30: 13641–13649, 2014. doi:10.1021/la503011u.
51. **Zanotti S, Gibertini S, Bragato C, Mantegazza R, Morandi L, Mora M.** Fibroblasts from the muscles of Duchenne muscular dystrophy patients are resistant to cell detachment apoptosis. *Exp Cell Res* 317: 2536–2547, 2011. doi:10.1016/j.yexcr.2011.08.004.